Micromesh-selection for the ATLAS New Small Wheel Micromegas detectors

Jinst

Published by IOP Publishing for Sissa Medialab

Received: *September 20, 2016*
Accepted: *November 22, 2016*
Published: *November 30, 2016*

18th International Workshop on Radiation Imaging Detectors
3–7 July 2016,
Barcelona, Spain

Micromesh-selection for the ATLAS New Small Wheel Micromegas detectors

F. Kuger on behalf of the ATLAS Muon collaboration

CERN
Geneva 23, Switzerland
University of Würzburg
97074 Würzburg, Germany

E-mail: Fabian.Kuger@cern.ch

Abstract: The ATLAS New Small Wheels will be the first major upgrade to an LHC experiment utilizing the Micromegas technology. With an active detection area of 1280 m^2 and comprising more than two million channels it is the largest and probably most ambitious system of Micro Pattern Gaseous Detectors (MPGDs) currently under construction.

The eponymous component of the Micromegas technology, the micromesh, is the detector's most precise component. Although a wide range of meshes, mesh geometries and parameters can be used to build an operational Micromegas, its properties can affect a range of detector qualities, such as reconstruction efficiency, timing and energy resolution. Conversely, the correct choice of this component will permit a wider range in operation parameters and optimize the detector performance.

Keywords: Materials for gaseous detectors; Micropattern gaseous detectors (MSGC, GEM, THGEM, RETHGEM, MHSP, MICROPIC, MICROMEGAS, InGrid, etc); Detector design and construction technologies and materials

[1]Corresponding author.

doi:10.1088/1748-0221/11/11/C11043

Contents

2016 JINST 11 C11043

1 Introduction

To fully exploit the discovery potential of the Large Hadron Collider [1], an upgrade towards high luminosity (HL-LHC) is scheduled for 2024-25 [2]. In parallel to the accelerator, the experiments have to be adapted to the higher luminosity, causing higher particle rates and detector occupancy [3]. Within the next long shutdown the innermost end-cap stations of the ATLAS Muon spectrometer [4] will be replaced by the New Small Wheels [5]. Each of them comprises resistive Micromegas and sTGC detectors in an overlapping structure of eight large and eight small sectors, with each sector hosting two (Micromegas) respectively three (sTGC) Quadruplet modules (4 active detection layers) (figure 1).

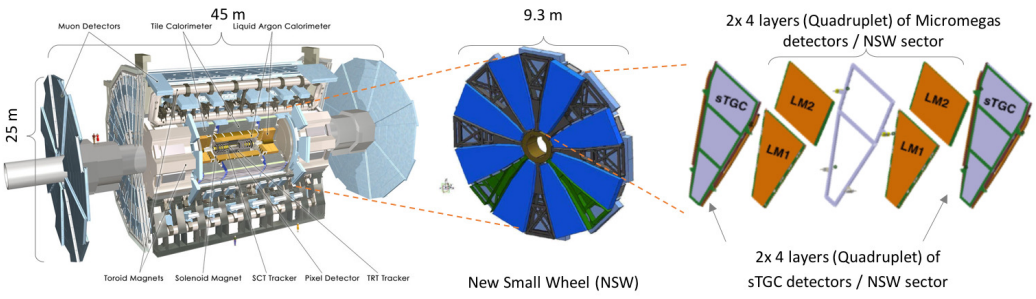

Figure 1. The ATLAS Detector at the LHC (left) [4] showing the position of the (New) Small Wheels with their sector structure (center) [5] and the composition of each sector out of sTGC and Micromegas Quadruplet modules (right).

A key component of the Micromegas (**Micromes**h **ga**seous **s**tructure) [6] detectors is the fine conductive mesh, dividing the gas volume into a drift and an amplification region. The selection of the proper mesh is an important design objective, affecting various detector aspects, several of these being discussed in this publication.

2 An ideal Micromesh for a Micromegas detector

The construction of m^2-size Micromegas detectors with a mechanically floating mesh[1] requires sufficient robustness of the meshes. Additionally they must be durable enough to sustain a sequence of assembly, transport and cleaning processes.

In an ideal Micromegas the cathode, the anode and the mesh create independent and homogeneous electrical fields in the drift and the amplification volume. Therefore the mesh should resemble to first approximation a metallic plane with an internal structure finer than all other detector components. It should be as thin and flat as possible.

On the other hand an ideal mesh would be completely permeable to electrons traversing from the low drift field into the amplification field region while absorbing all ions drifting in the other direction. Furthermore it should allow an unhindered gas exchange between the volumes. Both requirements support a highly perforated structure.

Since no material can fully satisfy all these partially contradicting requirements, a trade-off between the different aspects is required.

3 Mechanical and production-related considerations

Meshes or grids can be produced by a variety of techniques. Although photo-lithographical etching or electroforming can yield finer-pitched and flatter meshes, these grid structures typically lack the mechanical robustness to be stretched over several meters, as required for a large size floating mesh Micromegas. Weaving of stainless steel wires has proven to be the most reliable method to manufacture accurate and mechanically durable meshes of several m^2 size.

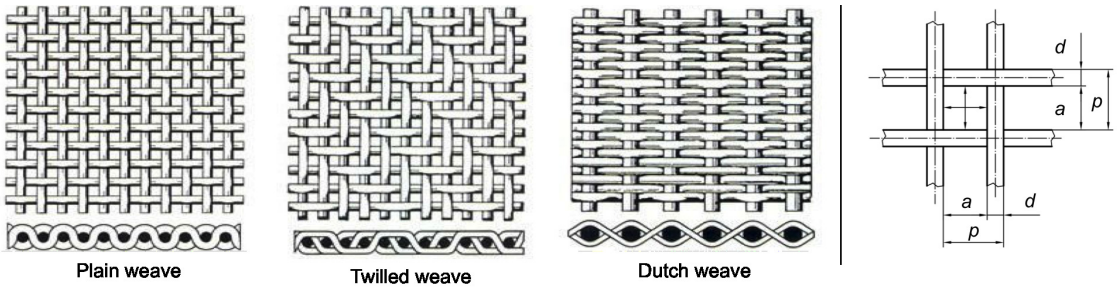

Figure 2. Left: schematic of the three most common weaving patterns: plain weave, twilled weave and (plain) dutch weave (left to right). Right: defining geometry of a plain weave unit cell. [7].

Different weaving patterns can increase the robustness of the mesh cloth but cause smaller open areas and/or asymmetries in warp and weft directions, like e.g. the dutch weave. Plain weave

[1]The mesh is stretched and positioned on a layer of support pillars. Once the anode is polarized the resulting electrostatic force draws the electrically grounded mesh on the pillars and creates a precise amplification gap.

2016 JINST 11 C11043

results in the symmetric pattern with shortest periodicity and represents the best approximation to a flat perforated plane (figure 2). For the symmetrical plain weave, the mesh is completely specified by the wire diameter d and the aperture between neighboring wires a (figure 2). The open area of the mesh is defined as $O = [a/(a+d)]^2$ and its pitch or periodicity is $p = a + d$.

The weaving process of meshes with more than two meter width requires sufficiently stable wires. Additionally a reduction of the wire diameter requires more wire-length to weave a mesh of comparable open area and thus increases costs per square meter significantly. To avoid production flaws and to keep costs reasonable, a wire diameter of $\geq 30\,\mu m$ is recommended. Choosing the mesh aperture for optimized mechanical properties is a trade-off: while smaller apertures increase the bending angle of the wire during the weaving process and therefore the risk of wire rapture, a mesh cloth with larger apertures is less rigid and more prone to damage during handling.

Although the flatness of the mesh can be increased by calendering, a process where the mesh cloth is pressed between two precisely parallel rolls, this process is not industrially available for meshes of $> 2\,m$ width.

4 Homogeneity of the amplification field and gas gain

Although primarily determined by the potential difference between the mesh and the anode the electrical field in the amplification gap, and thus the Micromegas gain, is highly sensitive to small changes in the electrodes' geometry and position. Figure 3 visualizes the electrical field in the amplification gap and the drift volume close to the mesh wires. The streamlines indicate the idealized electron path, neglecting diffusion in the gas. Electrons created in the drift volume are strongly focused on a path in-between the mesh wires and accordingly the electrical field strength along these paths is the main determinant for the Micromegas' gain.

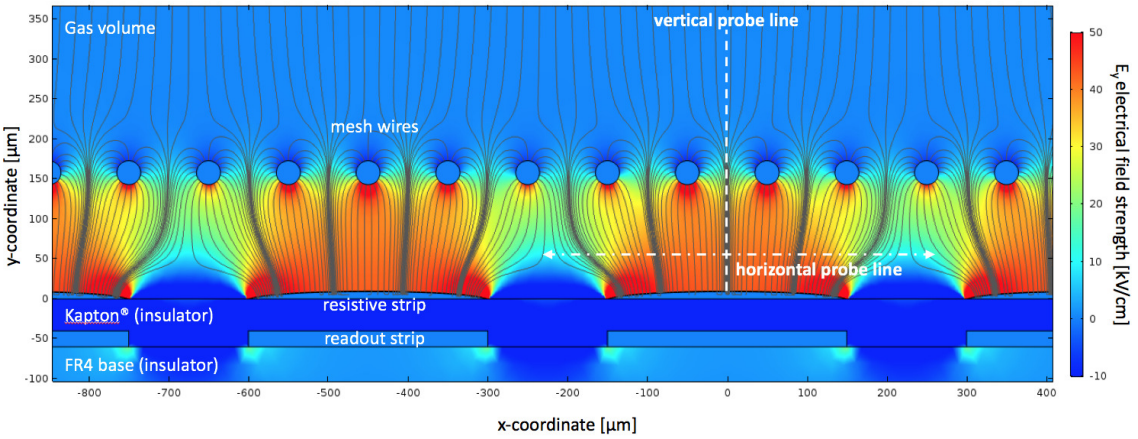

Figure 3. Electrical field strength in the vicinity of the mesh wires. The mesh has a periodicity of 100 µm (diameter = 30 µm, aperture = 70 µm), the strip pitch is 450 µm (strip width = 300 µm). The position and orientation of two probe lines are indicated (dashed). (COMSOL Multiphysics® [8] Simulation — the streamline (grey) density is not proportional to the field strength.)

With an increased distance between the wires, the electrical field strength along the electrons' most probable path through the amplification gap (vertical probe line) decreases as shown in

2016 JINST 11 C11043

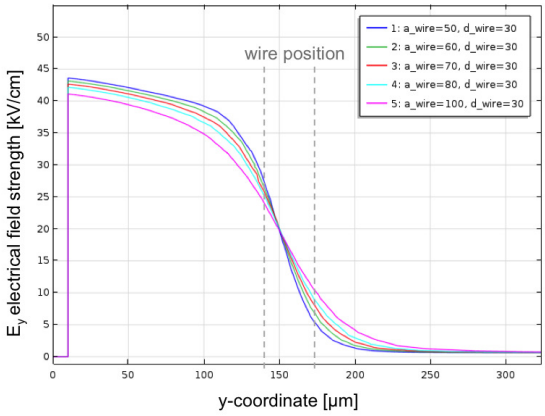

Figure 4. Electrical field strength along a vertical probe line through the amplification gap of a Micromegas with different mesh apertures.

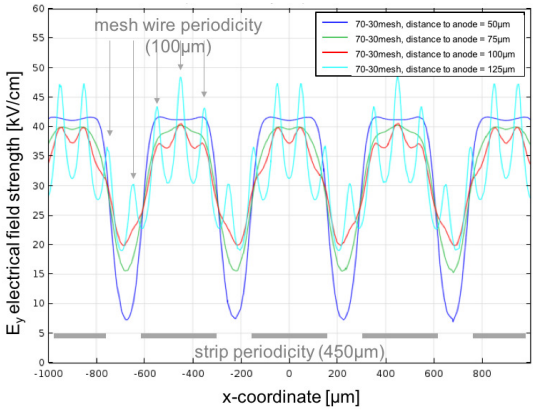

Figure 5. Electrical field strength fluctuation along a set of horizontal probe lines parallel to a mesh with 100 µm periodicity.

figure 4. Consequentially a larger aperture results in a smaller gas gain requiring higher voltages for comparable gain, increasing the risk of discharges in the detector.

The influence of the wire positions on the field homogeneity along the amplification gap (horizontal probe line) is clearly visible in figure 5 and most pronounced close to the wires. Along the wire periodicity, the non-homogeneity is dominated by the anode strip structure, especially in the lower part of the amplification gap.

5 Electrostatic shielding between drift- and amplification-field

Since a mesh is not a continuous metal plate, the electrical fields on both sides are not perfectly shielded, but interfere with each other. The shielding capabilities of different meshes can already be assessed in figure 4, depicting the significant deviation of the electrical field strength from the nominal drift field $E_{D,\mathrm{nom}}$ in the vicinity of the mesh wires. Besides this effect, which is locally constrained to the region of non-homogeneous drift fields close to the wires, a mesh specific deviation from nominal is visible closer to the drift cathode as well (figure 6). While a continuous offset between the effective drift field strength $E_{D,\mathrm{eff}}$ and its nominal value $E_{D,\mathrm{nom}}$ can easily be taken into account in a TPC-like reconstruction algorithm, the increase of the non-homogeneous region within the drift volume is more difficult to cope with. Hence, an aperture not wider than 80 µm between neighboring 30 µm wires is recommended, to limit the $E_{D,\mathrm{eff}}$ uncertainty in the top 80 % of the drift gap to ≤ 1 %.

The non-homogeneity along a horizontal direction in the drift volume, parallel to the mesh is shown in figure 7. It is dominated by the anode strip periodicity for distances ≥ 300 µm from the anode, ≈ 130 µm from the mesh top surface. The wires systematic effect on the electrical field strength is only visible closer to the mesh. For distances ≥ 500 µm from the anode, the field strength fluctuation is < 1 % $E_{D,\mathrm{eff}}$ for a mesh aperture of ≤ 70 µm.

A similar effect of the drift field on the field-strength in the amplification region can be observed, but is negligibly small due to the ratio of the two fields.

2016 JINST 11 C11043

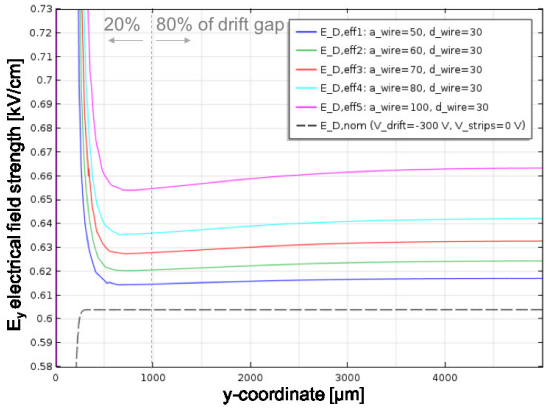

Figure 6. Electrical field strength along the drift gap of a Micromegas with different mesh apertures.

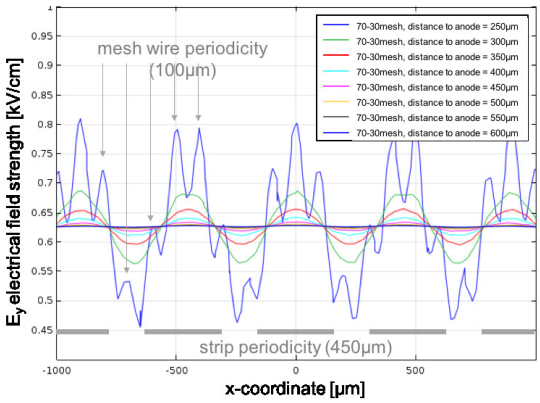

Figure 7. Electrical field strength fluctuation along parallel horizontal lines above a mesh with 100 µm periodicity.

6 Electron Transparency

Electrons approaching the mesh are either conducted through the mesh or end up on its surface due to scattering [9]. If absorbed by the mesh the electrons are lost for signal production. Consequently, an electron transparency close to 100 % is important for optimal track reconstruction.

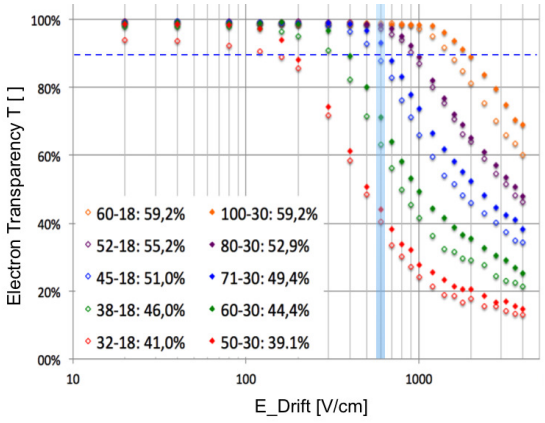

Figure 8. Electron transparency of different mesh geometries (mesh aperture - wire diameter: open area) as function of the drift field strength.

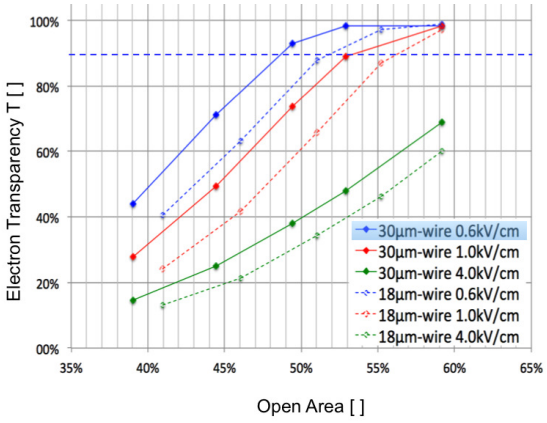

Figure 9. Electron transparency as function of the open area for 30 µm- and 18 µm-wire meshes and three drift field settings.

Figure 8 and figure 9 summarize extensive simulation studies on electron transparencies, verified by measurements with an exchangeable mesh Micromegas prototype [10]. With a 30 µm-wire an aperture of ≥ 70 µm (open area > 49 %) is required to reach an electron transparency of ≥ 90 % (dashed line) with the voltage settings foreseen for the NSW Micromegas (shaded blue region).

2016 JINST 11 C11043

7 Gas flow through the mesh

An effective gas exchange through the mesh is important to keep the gas mixture in the amplification gap pure, since contamination is created there during the avalanche formation e.g. by dissociative attachment: $e^- + CO_2 \rightarrow O^- + CO$. Gas-flow-simulations with a simplified (flat) mesh model ($d = 30\,\mu m$, $a = 70\,\mu m$) show a gas exchange time between drift and amplification volumes in the order of a few seconds (figure 10). Given the exchange-rate of the full detector (4 Volumes/day), the gas flow hindrance caused by the mesh is negligible.

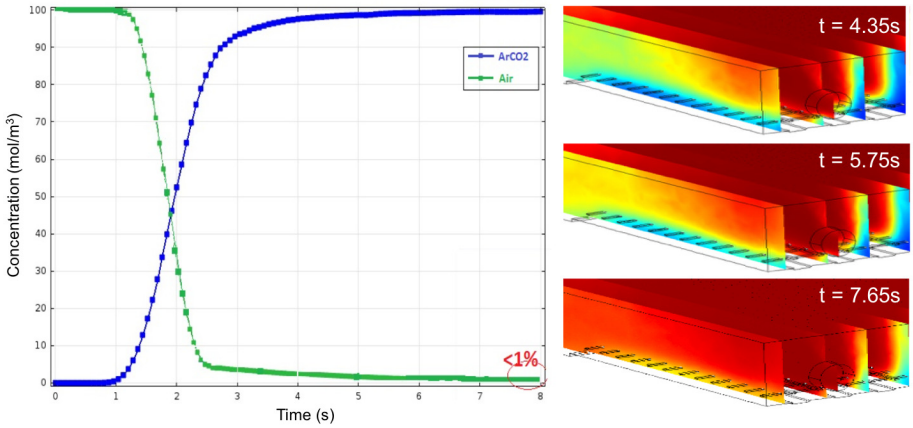

Figure 10. Propagation of the gas during the exchange process (blue: old gas; red: new gas) in the drift- and the amplification-region at three sequential instances.

8 Conclusion and Mesh-selection

Woven wire meshes have proven to be an affordable and technologically viable choice for large area Micromegas. Although a finer and flatter mesh is desirable, mechanical stability and cost-considerations exclude wires of $< 30\,\mu m$ diameter. The meshes' transparency to electrons (and to a certain extend also to the gas flow) requirements set a lower limit to the mesh aperture. Very large apertures are excluded because of the decrease in amplification field homogeneity and the increase in interference effects between the electrical fields.

A plain weave mesh with 71 µm aperture, 30 µm wire diameter and 250 lines per inch (lpi) is the optimum trade-off between all the above aspects. The large-scale production of 2800 m^2 woven wire mesh (71/30, 250 lpi) for the ATLAS NSW Micromegas has been finished in June 2016.

Acknowledgments

We express our thanks to our industrial partners, the mesh weaving companies BOPP, Haver & Boecker and PACO, for the knowledge transfer and their cooperativeness in technical and production-related questions.

2016 JINST 11 C11043

References

[1] L. Evans and P. Bryant, *LHC Machine*, 2008 *JINST* **3** S08001.

[2] ATLAS, CMS collaboration, K. Jakobs, *Physics at the LHC and sLHC*, *Nucl. Instrum. Meth.* **A 636** (2011) S1.

[3] D. Bortoletto, *The ATLAS and CMS Plans for the LHC Luminosity Upgrade*, arXiv:0809.0671.

[4] ATLAS collaboration, *The ATLAS Experiment at the CERN Large Hadron Collider*, 2008 *JINST* **3** S08003.

[5] ATLAS collaboration, *ATLAS New Small Wheel Technical Design Report*, ATLAS-TDR-020-2013, Geneva (2013).

[6] Y. Giomataris, P. Rebourgeard, J.P. Robert and G. Charpak, *MICROMEGAS: A High granularity position sensitive gaseous detector for high particle flux environments*, *Nucl. Instrum. Meth.* **A 376** (1996) 29.

[7] International Organization for Standardization, *Industrial woven wire cloth - Technical requirements and testing*, ISO 9044 (1999).

[8] COMSOL AB, *COMSOL Multiphysics v.5.5*, www.comsol.com, Stockholm, Sweden.

[9] K. Nikolopoulos, P. Bhattacharya, V. Chernyatin and R. Veenhof, *Electron transparency of a Micromegas mesh*, 2011 *JINST* **6** P06011.

[10] F. Kuger, M. Bianco, P. Iengo, G. Sekhniaidze, R. Veenhof and J. Wotschack, *Mesh geometry impact on Micromegas performance with an Exchangeable Mesh prototype*, *Nucl. Instrum. Meth.* **A 824** (2016) 541.

2016 JINST 11 C11043